Photosynthesis Research **78:** 67–76, 2003.

Regular paper

Photosynthetic and respiratory electron transport in the alkaliphilic cyanobacterium *Arthrospira (Spirulina) platensis*

S. Berry[1], Y.V. Bolychevtseva[2], M. Rögner[1,*] & N.V. Karapetyan[2]
[1]*Faculty of Biology, Ruhr University – Bochum, Universitätsstr. 150, 44780 Bochum, Germany;* [2]*A.N. Bakh Institute of Biochemistry, Russian Academy of Sciences, Leninsky pr. 33, 119071 Moscow, Russia;* **Author for correspondence (e-mail: matthias.roegner@ruhr-uni-bochum.de; fax +49-234-3214322)*

Received 13 February 2003; accepted in revised form 3 June 2003

Key words: fluorescence, proton translocation, sodium

Abstract

Photosynthetic and respiratory electron transport and their interplay with ion transport have been studied in *Arthrospira platensis*, a filamentous alkaliphilic cyanobacterium living in hypersaline lakes. As typical for alkaliphiles, *A. platensis* apparently does not maintain an outward positive pH gradient at its plasma membrane. Accordingly, sodium extrusion occurs via an ATP-dependent primary sodium pump, in contrast to the Na^+/H^+ antiport in most cyanobacteria. *A. platensis* is strongly dependent on sodium/bicarbonate symport for the uptake of inorganic carbon. Sodium extrusion in the presence of the Photosystem II inhibitor diuron indicates that a significant amount of ATP is supplied by cyclic electron transport around Photosystem I, the content of which in *A. platensis* is exceptionally high. Plastoquinol is oxidized by two parallel pathways, via the cytochrome b_6f complex and a putative cytochrome *bd* complex, both of which are active in the light and in the dark.

Abbreviations: AO – acridine orange; AY – acridine yellow; Chl chlorophyll *a* – ; Ci – inorganic carbon; Cyd – cytochrome *bd*-type quinol oxidase; cyt – cytochrome; DBMIB – 2,5-dibromo-6-isopropyl-3-methyl-1,4-benzoquinone; DCCD – N,N′dicyclohexylcarbodiimide; DCMU – 3-(3,4-dichlorophenyl)-1,1′-dimethylurea (= diuron); FCCP – carbonyl cyanide 4-trifluoromethoxyphenylhydrazone; F_0 – initial chlorophyll fluorescence from dark adapted cells; F_{max} – maximum chlorophyll fluorescence; F_v – variable chlorophyll fluorescence; HL/LL – high/low light; PCP – pentachlorophenol; PMS – phenazine methosulfate; P700 – primary electron donor of PS I; PQ – plastoquinone; PS – photosystem; Q_A – primary electron acceptor of PS II; *Synechocystis* 6803 – *Synechocystis* sp. PCC 6803; TCA – trichloroacetic acid; ΔpH – transmembrane pH difference; $\Delta\Phi$ – fluorescence change of acridine dye during illumination; Φ_S – stationary fluorescence of acridine dye in dark adapted cells

Introduction

Arthrospira (Spirulina) platensis (Mohanty et al. 1997; Vonshak 1997) is a filamentous cyanobacterium adapted to the environment of alkaline lakes. These habitats exhibit a high concentration of inorganic carbon (Ci) as carbonate, which is in principle advantageous to photoautotrophic organisms. However, soda lakes are characterized by high pH and high sodium concentration and, in some cases, by high solar light intensity (especially in shallow lakes) and elevated temperature. For this reason, studying the key bioenergetic processes in *A. platensis* cells is of relevance for understanding the adaptations of cyanobacteria and other bacteria to these extreme conditions.

Sodium/proton antiporters are the major mechanism for sodium extrusion and adaptation to salt stress in various cyanobacteria (Buck and Smith 1995; Elanskaya et al. 2002; Inaba et al. 2001; Waditee et al. 2002). This requires generation of a proton motive force (by respiration or ATP hydrolysis) at the plasma membrane, which is then converted into the sodium

gradient. The Na^+ gradient at the plasma membrane of cyanobacteria is crucial for photosynthesis, as sodium/bicarbonate symport is a major route for Ci uptake (Kaplan and Reinhold 1999; Li and Canvin 1998; Shibata et al. 2002).

While photosynthesis and respiration have already been investigated in *A. platensis* (Karapetyan et al. 1997; Karapetyan et al. 1999; Mohanty et al. 1997; Shubin et al. 1993; Vonshak 1997), especially with respect to the impact of salt stress (Lu and Zhang 2000; Lu et al. 1999; Schlesinger et al. 1996; Verma and Mohanty 2000; Zeng and Vonshak 1998), the knowledge of transport processes and ion homeostasis in this organism is still limited (Xu et al. 1994). In the present paper, we address the interplay of the bioenergetic processes in whole cells of *A. platensis*. As the genomic sequence is not yet available for this organism, and as there is also no established protocol for generating site-directed mutants, our approach is to use a range of inhibitors already established for other cyanobacteria to dissect the various bioenergetic pathways. To compensate for a potential unspecific action of these inhibitors we use a range of biophysical methods to obtain an overall picture encompassing a number of bioenergetic parameters. Our results indicate that sodium extrusion occurs via a primary Na^+-pump using ATP generated by PS I cyclic electron transport. Evidence is also presented for a cyt *bd*-type quinol oxidase operating in thylakoids in parallel to the cyt b_6f complex.

Materials and methods

Growth conditions and cell harvesting

A. platensis strain P 511 was obtained from the IPPAS Culture Collection of Microalgae, Institute of Plant Physiology, Russian Academy of Sciences. Cells were cultivated at 30 °C and a light intensity of 40 μE s^{-1} m^{-2} in *Spirulina* medium, pH 9.6 (Schlösser 1994) in aerobic 250 ml Erlenmeyer flask cultures which were shaken once every day. After 6 to 8 days cells were harvested by filtration through nylon gaze (Miracloth), resuspended and adjusted to 10 μg/ml Chl (5 μg/ml for 77 K chlorophyll fluorescence and 2.5 μg/ml for fluorescence induction). The suspension medium contained 5 mM $MgCl_2$ and either 2 mM NaCl, 100 mM NaCl or 100 mM KCl, respectively, buffered at pH 8 with TRICINE (2 mM for pH electrode measurements, 50 mM elsewhere; adjusted with NaOH for NaCl media, and KOH for KCl media, respectively).

Polarographic measurements

Photosynthetic oxygen evolution (at a light intensity of 1250 μE s^{-1} m^{-2}) and respiratory oxygen consumption were measured at 30 °C using the Oxy-Lab system from Hansatech (King's Lynn, UK). The irradiance was saturating for O_2 evolution and thus was comparable the HL illumination used elsewhere in this paper.

Induction of chlorophyll fluorescence

Fluorescence induction was measured in two time ranges, applying either one second or several minutes of illumination. The redox state of Photosystem II during several minutes of actinic illumination was monitored by pulse-amplitude modulated chlorophyll fluorescence with a PAM fluorometer (Walz, Effeltrich, Germany). Actinic red illumination (halogen lamp with Schott RG 630 glass filters and a Balzers Calflex-3000 heat protection filter) was used at either 406 μE s^{-1} m^{-2} (LL = low light) or 4060 μE s^{-1} m^{-2} (HL = high light). Short-term measurements provided information on the routes of plastoquinol oxidation in dark-adapted cells, which were illuminated for 1 second with blue light (205 μE s^{-1} m^{-2}, filter combination Schott GG 400 + Balzers DT-Blue). PS II fluorescence was monitored at 686 nm; illumination was controlled by an electronic shutter (rise time 2 milliseconds), with the fast phase of fluorescence rise during shutter opening attributed as F_0 (Berry et al. 2002).

Chlorophyll fluorescence spectra at 77 K

Fluorescence emission spectra were recorded by an Aminco Bowman 2 Spectrofluorometer (Spectronic Instruments, Rochester, New York, USA) to determine the state of PS I from the fluorescence intensity of the PS I trimers at 760 nm (Karapetyan et al. 1997; Shubin et al. 1993). Fluorescence was excited at 435 nm, and emission was recorded using a slit width of 4 nm. Spectra were corrected for the wavelength sensitivity of the instrument.

Change of extracellular proton concentration

For measurements with a pH electrode (Blue Line pH 12 from Schott, Mainz, Germany), a 4 ml cuvette was used with HL illumination as described above.

Acridine dye fluorescence

The fluorescence yield of acridine dyes depends on the local pH in cellular compartments; a pH decrease induces a parallel fluorescence decrease (Teuber et al. 2001). Dye concentration was 5 μM. A branched fiber optics was used for excitation and detection of fluorescence, using blue LEDs with filter combinations for excitation (Omega BP8 filters, 495 nm excitation/535 nm emission for AO and 445 nm/520 nm for AY).

Intracellular sodium content

Intracellular sodium was determined by flame photometry according to (Bakker and Harold 1980). 1.5 ml cell suspension were centrifuged (13000 rpm, 15 min) through 0.2 ml of low-viscosity silicone oil (DC 702 with 15% n-octane). Supernatant and silicone oil were carefully removed by a pipette and the pellet was extracted with 10% TCA (w/v) over night at room temperature. After a second centrifugation, the sodium concentration in the TCA extract was determined in an AAS30 flame photometer (Analytik, Jena, Germany). Averages for all measurements in this work are given as average ± standard deviation from at least three measurements.

Chemicals

Substances (usually at analytical grade) were obtained from Acros (Geel, Belgium: Monensin, sodium orthovanadate), J.T. Baker (Deventer, The Netherlands: All salts for cultivation and suspension media, TCA), Lancaster (Eastgate, UK: DCMU, PMS), Merck (Darmstadt, Germany: TRICINE) or Sigma-Aldrich/Fluka (Steinheim, Germany: Antimycin A, AO, AY, DBMIB, DCCD, FCCP, PCP, quinidine, silicone oil DC 702).

Results

Oxygen exchange measurements using cells of the cyanobacterium *Arthrospira platensis* under various conditions were performed to yield information on the activity of photosynthetic and respiratory electron transport routes. The rate of photosynthesis as determined from the rate of oxygen evolution in the light (Table 1) was about five times higher than the rate of respiration in the dark, which is typical of cyanobacteria (Schmetterer 1994). Addition of 10 mM sodium bicarbonate to a NaCl medium stimulated the photosynthetic rate only slightly (8%). Replacing NaCl by KCl caused the photosynthetic rate to decline to 77%, with a similar decrease in the rate of respiration. A saturating concentration of the cyt b_6f inhibitor DBMIB abolished net oxygen evolution, resulting in an oxygen consumption in the light which was equal to respiration in the dark. This rate of respiration amounted to 50% of the control, and oxygen consumption in the presence of DBMIB was still 2.5 times higher than the residual non-respiratory oxygen uptake (13 ± 5 μmol O_2 / mg Chl × h), which was observed in the presence of KCN, an inhibitor of all cyanobacterial respiratory oxidases (Schmetterer 1994). These results indicate an alternative pathway for plastoquinol oxidation bypassing the cyt b_6f complex. Oxygen evolution during illumination would then still occur in the presence of DBMIB, but be masked by an equivalent respiratory oxygen consumption.

Table 1. Polarographic determination of oxygen exchange. A positive value indicates oxygen evolution, a negative value consumption; respiratory rates in the dark were determined after five minutes illumination of the samples

Conditions	Rate of oxygen exchange / μmol O_2 (mg Chl × h)$^{-1}$	
	Light	Dark
100 mM NaCl	282±53	−64±19
100 mM NaCl + 10 mM $NaHCO_3$	305±64	−62±29
100 mM NaCl + 50 μM DBMIB	−27±6	−33±1
100 mM KCl	216±48	−45±16

To supplement the oxygen measurements Q_A, the primary quinone acceptor of PS II, was used as an indicator for photosynthetic electron transport; its redox state was estimated from the yield of variable chlorophyll fluorescence (Table 2). During HL illumination in the presence of NaCl, 80% of Q_A were reduced. Addition of bicarbonate caused a 10% decline of Q_A reduction, while switching to a KCl medium caused a 10% increase. Under LL the reduced fraction of Q_A increased even more when NaCl was replaced by KCl

Table 2. Determination of the redox state of Q_A under various conditions as estimated from chlorophyll fluorescence using a PAM fluorometer: $Q_A^{red}/\% = (F_v - F_0) / (F_{max} - F_0)$. Two values without standard deviation in the third column result from single determinations

Conditions	$Q_A^{red}/\%$	
	LL	HL
100 mM NaCl	26±13	80±1
100 mM NaCl + 10 mM $NaHCO_3$	23±10	69±3
100 mM NaCl + 1.25 mM DCCD	35±15	81
100 mM NaCl + 100 μM quinidine	70±21	n.d.
100 mM KCl	49±4	89

(i.e., LL conditions are more sensitive to monitor these salt effects on Q_A), and the sodium channel blocker quinidine (Allakhverdiev et al. 2000) similarly caused a high percentage of closed PS II. Only a moderate increase of Q_A reduction was achieved in the NaCl medium, when proton efflux from the thylakoids via the ATPsynthase was inhibited by DCCD. In conclusion, KCl as well as quinidine may block the electron efflux from PS II, leading to more reduced Q_A at room temperature.

In *A. platensis*, about 80% of all PS I complexes exist as trimers (Rakhimberdieva et al. 2001); they show a characteristic fluorescence band at 760 nm, the intensity of which is proportional to the fraction of reduced P700 both in isolated complexes (Karapetyan et al. 1997; Shubin et al. 1993) and whole cells (Kruip et al. 1999; Rakhimberdieva et al. 2001). Therefore, intensity changes of the 760 nm fluorescence may indicate either a shift of the trimer/monomer distribution of PS I, or a change of the redox state of P700 in trimers. 77 K chlorophyll fluorescence spectra of dark- and light-adapted cells were recorded with the cells being preincubated in either 100 mM NaCl or KCl under light or dark conditions, followed by quick freezing to fix the redox state of the electron transport cofactors (Figures 1A or 1B, respectively). A marked difference between NaCl- and KCl-incubated cells occurs with respect to the peak at 760 nm, which decreased strongly in both dark- and light-adapted cells in the potassium medium. This effect was simulated for light-adapted cells in the NaCl medium by addition of quinidine (Figure 1B). The decrease of the 760 nm peak in the presence of quinidine is accompanied by a rise of the 695 nm peak that reflects the redox state of Q_A (Papageorgiou 1996). This inverse correlation between the two peaks probably indicates a limited electron flow from PS II to PS I (see also discussion). Note that Q_A was more reduced in the presence of quinidine also at room temperature (Table 2).

The redox state of the PQ-pool, which can be monitored by fluorescence induction (Berry et al. 2002), is an indicator for photosynthetic and respiratory pathways, as it depends in the dark on the balance of oxidation and reduction processes by respiratory complexes. Most of the variable PS II fluorescence was quenched when dark-adapted cells were illuminated (Figure 2A, lower curve), due to the rapid photooxidation of the PQ pool and Q_A by PS I. (Maximum fluorescence yield was determined from a second illumination after addition of DCMU, which blocks electron transfer from Q_A to the PQ pool and induces complete reduction of Q_A). In the presence of DBMIB (Figure 2B) the variable fluorescence reached a higher level, indicating a significantly slowed down plastoquinol oxidation. An even faster and higher increase of F_v was observed after preincubation with DBMIB + KCN (Figure 2C), indicating now an almost completely reduced PQ pool in the dark. Corresponding with the respiration data (Table 1), which suggested a DBMIB-insensitive route for plastoquinol oxidation alternative to the cyt b_6f complex, Figure 2D indicates the presence of a cyt *bd* (Cyd) quinol oxidase, as the Cyd inhibitor PCP (Pils et al. 1997) had the same effect as KCN. In contrast, the separate effects of KCN or PCP were rather small (Figures 2E and 2F).

To monitor proton translocation coupled to electron transport, we used acridine dyes which indicate pH changes in whole cells (Teuber et al. 2001). Acridine orange (AO) was readily taken up by the cells (not shown); subsequent actinic illumination of cells preincubated with AO produced a rapid fluorescence decrease ($\Delta\Phi$), indicating acidification of the thylakoid lumen, which partially reverted after light off (Figures 3A and 3B). There was no indication of a fluorescence increase during illumination, which would indicate alkalization of the cytoplasm. This is a unique feature of *A. platensis*, as shown by comparison with two other species, *Synechocystis* 6803 (Figure 3C) and *Synechococcus elongatus* (Figure 3D).

The relative quenching of dye fluorescence was $\Delta\Phi/\Phi_S = 31 \pm 9\%$ in the presence of 100 mM NaCl, and $39 \pm 13\%$ in the presence of 100 mM KCl, i.e., cells incubated with potassium appear to sustain a larger proton gradient across the thylakoid membrane. This effect was specifically due to the absence of so-

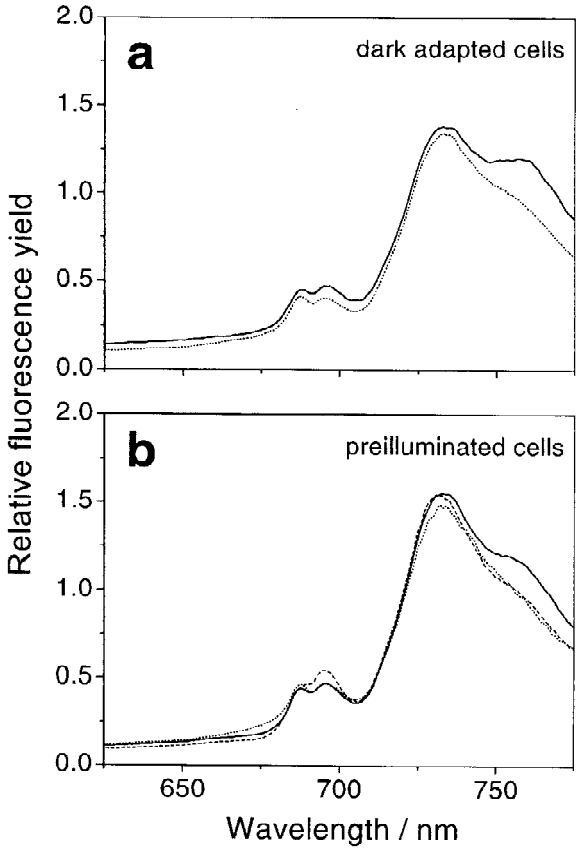

Figure 1. Chlorophyll fluorescence emission spectra of dark adapted (20 min) (A) or preilluminated (10 min) (B) cells. 5 μg Chl/ml in 100 mM NaCl (solid lines), 100 mM KCl (dotted lines), or 100 mM NaCl + 100 μM quinidine (dashed line in B). Cells were shock-frozen in liquid nitrogen. Each spectrum represents the average of four samples.

dium, since we found a light-induced $\Delta\Phi/\Phi_S = 25 \pm 7\%$ in a medium containing both 100 mM NaCl and 100 mM KCl, which is closer to the value obtained in the sodium-only medium. Further effects of various compounds on the light-induced $\Delta\Phi$ are shown in Table 3. The protonophoric uncouplers FCCP and nigericin completely abolished the signal, while the artificial electron acceptor PMS, which supports an proton-pumping cyclic electron transport at a high rate, induced a strong increase of $\Delta\Phi$. Both effects confirm that light-induced changes of AO fluorescence can be used to monitor specifically the proton gradient at the thylakoid membrane of *A. platensis*. Although the PS II inhibitor DCMU strongly decreased the signal, some proton translocation was still observed, indicating that the PS I cycle alone can generate a ΔpH. Accordingly, antimycin A, which blocks cyc-

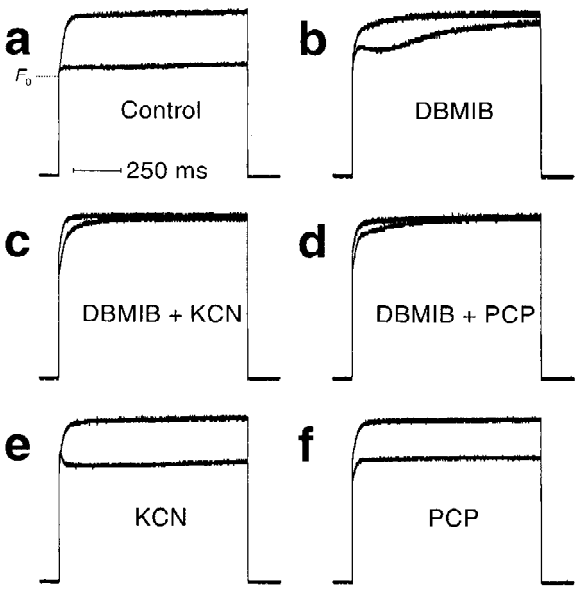

Figure 2. Fluorescence induction curves for monitoring electron transport routes. Each panel shows two curves, of which the lower was recorded in the presence of the indicated additions. The upper curve is the reference signal showing the full yield of F_V, obtained from a second illumination after addition of 10 μM DCMU. Before illumination cells (2.5 μg Chl/ml in a medium of 100 mM NaCl, 5 mM $MgCl_2$, 50 mM TRICIN, pH 8) were 5 min dark incubated under the following conditions: no additions (A), with 50 μM DBMIB (B), 50 μM DBMIB + 1 mM KCN (C), 50 μM DBMIB + 1 mM PCP (D), 1 mM KCN (E) or 1 mM PCP (F).

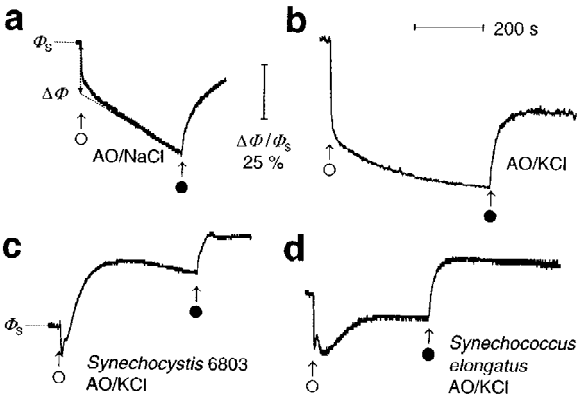

Figure 3. Light-induced fluorescence changes of acridine orange indicating pH-changes in whole cells. Cells were dark incubated with the dye for 20 min to obtain a stable baseline for Φ_S. Beginning and end of actinic HL illumination are indicated by open and closed circles. (A, B): Fluorescence change of AO in cell suspensions containing 100 mM NaCl (A) or 100 mM KCl (B). Due to the slow drift of the signal in the light, $\Delta\Phi$ was extrapolated to the onset of illumination. (C, D): Fluorescence change of AO in other cyanobacteria (see Teuber et al. 2001 for details). Scales for time and fluorescence quenching are identical for all panels.

Table 3. Effect of compounds affecting proton and electron transport reactions. Recorded was the light-induced fluorescence decrease of acridine orange, which indicates the acidification of the thylakoid lumen. The signal obtained under control conditions (100 mM NaCl, average $\Delta\Phi/\Phi_S$ = 31%, see Figure 3A) was used for normalization. Cells were preincubated with the dye in the dark for 20 min and illuminated with HL for 5 min

Conditions	Relative amplitude of AO signal
100 μM antimycin A	38±8%
50 μM DBMIB	39±13%
50 μM DBMIB + 1 mM PCP	0±0%
1.25 mM DCCD	134±21%
10 μM DCMU	23±8%
100 μM FCCP	0±0%
100 μM nigericin	0±0%
100 μM PMS	177±6%
100 μM quinidine	109±11%
1 mM sodium orthovanadate	129±28%

Table 4. Rate of extracellular alkalization during HL illumination (10 μg Chl/ml, 2 mM TRICIN) under various conditions as determined by a pH electrode. Samples were illuminated for 3 min; during this time the buffer capacity of the medium changed by less than 7%. The change of proton concentration was calibrated by adding small aliquots of a HCl standard to the sample after illumination

Medium containing	Additions	Rate μmol H^+ (mg Chl × h)$^{-1}$
2 mM NaCl	–	56±46
100 mM NaCl	–	248±43
100 mM NaCl	10 mM $KHCO_3$	349±6
100 mM NaCl	10 mM $KHCO_3$ + 50 μM DBMIB	0±0
100 mM NaCl	10 mM $KHCO_3$ + 1.25 mM DCCD	208±82
100 mM NaCl	10 mM $KHCO_3$ + 10 μM DCMU	0±0
100 mM NaCl	10 mM $KHCO_3$ + 100 μM quinidine	157±37
100 mM NaCl	10 mM $KHCO_3$ + 1 mM Na_3VO_4	93±5
100 mM KCl	–	27±27

lic electron transport (Endo et al. 1998), significantly decreased the AO signal. DBMIB did not completely suppress ΔpH formation even at saturating concentrations, while DBMIB supplemented by PCP did, confirming the presence of a cyt *bd*-type oxidase. Two ATPase inhibitors caused an increase of $\Delta\Phi$: In case of DCCD, this is in agreement with the expected decreased proton efflux from the thylakoid lumen. However, the effect of orthovanadate must be indirect, being an inhibitor of P-type ATPases in the plasma membrane. Quinidine had a smaller effect. Another dye, acridine yellow, confirmed all these effects (not shown), but it had a signal amplitude 2.5 times smaller than AO and provided no additional information.

The rate of Ci-uptake was monitored by the stationary rate of external alkalization during illumination, caused by the disappearance of CO_2 from the medium (Table 4). In the presence of 100 mM NaCl this rate increased significantly (41%) by addition of 10 mM potassium bicarbonate. A lowered sodium concentration (2 mM NaCl) yielded only 23% of the high-sodium value, which decreased to 11% in the complete absence of sodium (100 mM KCl). The effects of ion composition and of added hydrogen carbonate on the rate of Ci-uptake are thus more pronounced than those on the net rate of oxygen evolution (compare with Table 1). In the presence of two inhibitors of photosynthesis, DBMIB and DCMU, no Ci uptake was observed; presumably CO_2 fixation was also blocked under these conditions. The P-ATPase inhibitor orthovanadate (Peschek et al. 1988), the F-ATPase inhibitor DCCD, and the channel blocker quinidine showed somewhat smaller inhibitory effects.

Finally, the effects of various compounds on the intracellular sodium concentration were investigated (Table 5). Since the cells were incubated at high external sodium concentration, any compound interfering with sodium extrusion is expected to increase the intracellular sodium content. The largest effect was observed for DCCD, which blocked phosphorylation, i.e., the energy supply for sodium pumping. Also, the Na^+-ionophore monensin, which induces the collapse of a sodium gradient, and orthovanadate showed a strong effect. Quinidine had no effect, implying that its above reported effects are not due to interference with active sodium pumping. DCMU has no effect on sodium extrusion; this is to be expected because respiratory electron transport alone must be sufficient to maintain the sodium gradient, especially at night. In the light, there would be also DCMU-insensitive cyclic electron transport around PS I to provide energy for sodium extrusion. DBMIB caused a moderate increase of the sodium content, suggesting that the re-

Table 5. Relative cellular sodium concentration after incubation of the cells for one hour at an illumination of 40 μE s^{-1} m^{-2} (10 μg Chl/ml in buffer medium containing 100 mM NaCl, 5 mM MgCl2, 50 mM TRICIN, pH 8). Sodium content of the control cells (used as 100% reference for normalization) was 21 6 mol Na/mol Chl (6 determinations). Data obtained by flame photometry after silicone oil centrifugation and subsequent TCA extraction

Conditions	Relative cellular sodium content
50 μM DBMIB	215±53%
1.25 mM DCCD	565±19%
10 μM DCMU	103±12%
100 μM monensin	444±36%
100 μM quinidine	116±8%
1 mM sodium orthovanadate	359±97%

sidual electron transport via the cyt *bd* complex can generate a significant amount of ATP.

Discussion

Cyanobacteria contain two interacting membranes (Mohanty et al. 1997; Peschek 1999; Schmetterer 1994; Teuber et al. 2001): The thylakoid membrane, combining photosynthetic and respiratory electron transport, and the plasma membrane, harboring a respiratory chain and various transporters for ion homeostasis and nutrient uptake. This flexible bioenergetic toolbox enables cyanobacteria to survive under a broad range of ecological conditions. Comparing the results presented here with published data, the following conclusions can be drawn with respect to *Arthrospira platensis*.

Physiological effects of salt stress have been studied previously in *Arthrospira* strains (Lu and Zhang 2000; Lu et al. 1999; Verma and Mohanty 2000; Vonshak 1997; Zeng and Vonshak 1998), but the mechanisms of sodium extrusion have not yet been addressed in detail. A vanadate-sensitive ATPase, showing a pH optimum in the alkaline region and a stimulation of ATP hydrolysis by Na^+ and K^+, was detected in isolated plasma membranes of *A. platensis* (Xu et al. 1994); our results presented here identify this ATPase as the major route for sodium pumping in *A. platensis*. Vanadate and the Na-ionophor monensin caused a strong increase of the cellular sodium content (Table 5), with vanadate additionally increasing the pH gradient at the thylakoid membrane (Table 3). While no vanadate-sensitive ATPase is expected in thylakoids, Na^+ dependent ATP hydrolysis at the plasma membrane obviously induces a high rate of photophosphorylation and by this contributes indirectly to a lower thylakoid ΔpH. Therefore, orthovanadate, by blocking a Na-ATPase, indirectly increases the thylakoid pH gradient to the same extent as DCCD, which directly blocks the thylakoid ATP synthase. A crucial mechanism for sodium extrusion thus seems to be a primary sodium pump, in contrast to most cyanobacteria, where ΔpH-dependent Na^+/H^+ antiport is the major adaptation to high salinity (Buck and Smith 1995; Elanskaya et al. 2002; Inaba et al. 2001; Waditee et al. 2002).

Both acridine dyes tested here, acridine orange (Figure 3, Table 3) and acridine yellow (not shown), showed a fluorescence decrease upon pumping of protons into the thylakoid lumen. However, irrespective of the suspension medium (NaCl or KCl), illumination did not induce a fluorescence increase corresponding to the alkalization of the cytoplasm, while such a biphasic time-course occurs in all other tested cyanobacteria (Barsky et al. 1981; Matthijs et al. 1985; Teuber et al. 2001) (see Figures 3C and D). This absence of a cytoplasmic alkalization may be due to an inverted pH gradient at the plasma membrane, as known from other alkaliphiles (Albers et al. 2001; Skulachev 1994). A quantitative interpretation, i.e., the calculation of absolute pH values, is complicated for acridine dye signals, especially with whole cells (Teuber et al. 2001). This drawback is compensated by the fact that the method is non-invasive and can be applied easily to monitor processes in whole cells. To our knowledge, this is the first report on pH-dependent acridine fluorescence quenching in A. platensis: It shows that it is possible to obtain reproducible signals from *A. platensis* cells which can be reasonably interpreted within the context of the other data. Merits and limits of this method for *A. platensis* have to be evaluated in further investigations; it is possible that the signals in *A. platensis* differ from the other cyanobacteria due to different cell morphologies.

Our results show that incubation of the cells in KCl medium under light or dark conditions caused an accumulation of reduced Q_A in PS II (Table 2, Figure 1). At the same time the fluorescence intensity at 760 nm in the 77K spectra decreased (Figures 1A and B). The latter effect may in principle either indicate a more oxidized state of P700, or a shift of the trimers towards the less active monomeric form of PS I

(Karapetyan et al. 1997; Kruip et al. 1999; Rakhimberdieva et al. 2001; Shubin et al. 1993). However, for dark incubated cells it would be difficult to imagine how P700 could be oxidized and thus it seems likely that in both light and dark adapted cells an increase of the monomeric form of PS I occurred. Both such a downregulation of PS I activity and the accumulation of reduced Q_A point to a limitation of intersystem electron transport. The addition of the sodium channel inhibitor quinidine (Table 2, Figure 1B) in 100 mM NaCl medium perfectly simulated these effects: Both the yield of variable fluorescence (Table 2) and the fluorescence intensity at 695nm (Figure 1B) of *Arthrospira* cells increased in the presence of quinidine, and fluorescence intensity at 760 nm decreased. Furthermore, addition of quinidine to a sodium medium, like sodium depletion, strongly suppressed Ci uptake (Table 4). These results indicate the crucial importance of sodium/bicarbonate symport in *A. platensis* similar to other cyanobacteria (Kaplan and Reinhold 1999; Li and Canvin 1998; Shibata et al. 2002). Quinidine has been reported to block the entry of sodium in *Synechococcus* sp. cells (Allakhverdiev et al. 2000). Additionally, there is evidence that quinidine can inhibit Na^+-coupled solute uptake in *Synechocystis* 6803 (Berry et al. 2003), and so this substance is an interesting candidate for future studies of Na^+ bioenergetics in cyanobacteria in general. However, further tests would be desirable to exclude an inhibitory action on any of the photosynthetic complexes. Nevertheless, the data presented here indicate that quinidine induced no increase of the intracellular sodium content (Table 5), i.e. it did not interfere with the reactions involved in sodium extrusion in *A. platensis*. Ci uptake was also considerably inhibited by orthovanadate (Table 4), indicating that ATP-driven sodium extrusion and Na^+-coupled Ci uptake are the major components of a sodium cycle at the plasma membrane. The effects of sodium limitation or NaCl + quinidine on photosynthetic electron transport may be primarily due to pH control because of a low Na^+-ATPase activity at the plasma membrane, similar to the action of vanadate.

While higher plants show a PS I/PS II ratio close to unity, PS I is much more abundant in cyanobacteria: In *A. platensis* about 95% of total chlorophyll is associated with PS I, and the stoichiometry of PS I/PS II is particularly high reaching 5.5 (Rakhimberdieva et al. 2001). From this, an important contribution of a PS I cycle to the cellular energetics would be expected. This is in line with a strict ATP requirement for sodium extrusion and is in contrast with other cyanobacteria, which may alternatively utilize NADPH for sodium extrusion (Na^+/H^+ antiport driven by respiratory proton pumping at the plasma membrane (Peschek et al. 1988; Teuber et al. 2001)). In fact, the PS II inhibitor DCMU did not completely prevent the light-induced formation of a thylakoid ΔpH in *A. platensis* (Table 3), and the capacity of the PS I cycle for efficient ATP synthesis was indicated by the absence of a DCMU-inhibition of sodium extrusion (Table 5). Also, Antimycin A, blocking cyclic electron transfer at the level of the PQ reduction (Endo et al. 1998), significantly lowered the thylakoid ΔpH.

Four lines of evidence indicate a plastoquinol oxidation process, which can bypass the cyt b_6f complex: (1) The cyt b_6f inhibitor DBMIB suppressed photosynthetic net O_2 evolution, but not respiratory O_2 consumption (Table 1); the residual oxygen consumption in the presence of DBMIB could, in principle, also be due to a diaphorase reaction that is catalyzed by ferredoxin:NADP oxidoreductase (Bojko and Wieckowski 1995). However, as two different inhibitors of respiratory oxidases inhibit plastoquinol oxidation in the presence of DBMIB completely (see below), it seems more plausible to attribute this oxygen consumption to such an oxidase. (2) In the presence of DBMIB, part of the variable fluorescence was quenched during illumination, indicating a partial oxidation of the PQ pool. In contrast, the combination of DBMIB with the cyt *bd* inhibitor PCP or with KCN, an inhibitor of all respiratory oxidases, completely suppressed F_v quenching and induced complete PQ reduction in the dark by respiratory dehydrogenases (Figure 2). (PCP or KCN alone did not block photosynthetic electron transport, Figures 2E, F). (3) DBMIB did not fully suppress light-induced thylakoid acidification, while the combination of DBMIB and PCP did (Table 3). (4) DBMIB did not inhibit sodium extrusion completely, i.e., electron transport sustaining ATP synthesis persists in the presence of this inhibitor (Table 5). An alternative electron transport via Cyd is the most likely explanation for these observations. The operation of this quinol oxidase has been investigated thoroughly in *Synechocystis* 6803 (Berry et al. 2002; Büchel et al. 1998; Howitt et al. 1999; Pils et al. 1997; Pils and Schmetterer 2001). Although its detailed function is still unknown, it could act as a "valve" for excess electrons and by this may be useful especially under stress conditions. In *A. platensis*, the significant activity of this pathway may be related to its extreme environment.

In conclusion, the investigations of this report may contribute to a better understanding of the complex network of bioenergetic processes in the cytoplasmic membrane, the thylakoid membrane and the cytoplasm. Comparisons of these processes between various cyanobacterial strains reveal similarities, such as the increasing evidence for the role of an alternative oxidase, the cyt *bd* complex. On the other hand, they also show special strategies and adaptations of strains like *A. platensis* for extreme environments – in this case alkaline and hypersaline – which are mainly realized by using available components from the "toolbox" with different expression levels. This confirms the versatility of cyanobacterial gene equipment and may be the major reason for their global distribution.

Acknowledgements

This study was supported by the Deutsche Forschungsgemeinschaft (SFB 480/TP C1, S.B. and M.R.), a NATO Collaborative Linkage Grant (LST.CLG.978304), and The Russian Foundation of Basic Research (grant 02-04-48348, N.V. and Y.B.). S.B. acknowledges Berndt Esper, Bochum, for his introduction to the flame photometer.

References

Albers SV, Van de Vossenberg JL, Driessen AJ and Konings WN (2001) Bioenergetics and solute uptake under extreme conditions. Extremophiles 5: 285–294

Allakhverdiev SI, Sakamoto A, Nishiyama Y, Inaba M and Murata N (2000) Ionic and osmotic effects of NaCl-induced inactivation of Photosystems I and II in *Synechococcus* sp. Plant Physiol 123: 1047–1056

Bakker EP and Harold FM (1980) Energy coupling to potassium transport in *Streptococcus faecalis*. Interplay of ATP and the protonmotive force. J Biol Chem 255: 433–440

Barsky EL, Gusev MV, Nikitina KA and Samuilov VD (1981) Light-induced proton translocation through thylakoid and cytoplasmic membranes of *Plectonema boryanum*. Arch Microbiol 129: 105–108

Berry S, Schneider D, Vermaas WFJ and Rögner M (2002) Electron transport routes in whole cells of *Synechocystis* sp. strain PCC 6803: The role of the cytochrome *bd*-type oxidase. Biochemistry 41: 3422–3429

Berry S, Esper B, Karandashova I, Teuber M, Elanskaya I, Rögner M and Hagemann M (2003) Potassium uptake in the unicellular cyanobacterium *Synechocystis* sp. strain PCC 6803 mainly depends on a Ktr-like system encoded by *slr1509 (ntpJ)*. FEBS Lett 548: 53–58.

Bojko M and Wieckowski S (1995) Diaphorase activity of ferredoxin: NADP oxidoreductase in the presence of dibromothymoquinone. Phytochemistry 40: 661–665

Büchel C, Zsíros O and Garab G (1998) Alternative cyanide-sensitive oxidase interacting with photosynthesis in *Synechocystis* PCC6803. Ancestor of the terminal oxidase of chlororespiration? Photosynthetica 35: 223–231

Buck D and Smith G (1995) Evidence for a Na^+/H^+ electrogenic antiporter in an alkaliphilic cyanobacterium *Synechocystis*. FEMS Microbiol Lett 128: 315–320

Elanskaya IV, Karandashova IV, Bogachev AV and Hagemann M (2002) Functional analysis of the Na^+/H^+ antiporter encoding genes of the cyanobacterium *Synechocystis* PCC 6803. Biochemistry (Moscow) 67: 432–440

Endo T, Shikanai T, Sato F and Asada K (1998) NAD(P)H dehydrogenase-dependent, antimycin A-sensitive electron donation to plastoquinone in tobacco chloroplasts. Plant Cell Physiol 39: 1226–1231

Howitt CA, Udall PK and Vermaas WFJ (1999) Type 2 NADH dehydrogenases in the cyanobacterium *Synechcocystis* sp. Strain PCC 6803 are involved in regulation rather than respiration. J Bacteriol 181: 3994–4003

Inaba M, Sakamoto A and Murata N (2001) Functional expression in *Escherichia coli* of low-affinity and high-affinity Na^+ $(Li^+)/H^+$ antiporters of *Synechocystis*. J Bacteriol 183: 1376–1384

Kaplan A and Reinhold L (1999) CO_2 concentrating mechanisms in photosynthetic microorganisms. Annu Rev Plant Physiol Plant Mol Biol 50: 539–570

Karapetyan NV, Dorra D, Schweitzer G, Bezsmertnaya IN and Holzwarth AR (1997) Fluorescence spectroscopy of the long-wave chlorophylls in trimeric and monomeric Photosystem I core complexes from the cyanobacterium *Spirulina platensis*. Biochemistry 36: 13830–13837

Karapetyan NV, Holzwarth AR and Rögner M (1999) The Photosystem I trimer of cyanobacteria: Molecular organization, excitation dynamics and physiological significance. FEBS Lett 460: 395–400

Kruip J, Bald D, Boekema E and Rögner M (1994) Evidence for the existence of trimeric and monomeric Photosystem I complexes in thylakoid membranes from cyanobacteria. Photosynth Res 40: 279–286

Kruip J, Karapetyan NV, Terekhova IV and Rögner M (1999) *In vitro* oligomerization of a membrane protein complex. Liposome-based reconstitution of trimeric Photosystem I from isolated monomers. J Biol Chem 274: 18181–18188

Li Q and Canvin DT (1998) Energy sources for HCO_3^- and CO_2 transport in air-grown cells of *Synechococcus* UTEX 625. Plant Physiol 116: 1125–1132

Lu C and Zhang J (2000) Role of light in the response of PS II photochemistry to salt stress in the cyanobacterium *Spirulina platensis*. J Exp Bot 51: 911–917

Lu CM, Torzillo G and Vonshak A (1999) Kinetic response of Photosystem II photochemistry in the cyanobacterium *Spirulina platensis* to high salinity is characterized by two distinct phases. Aust J Plant Physiol 26: 283–292

Matthijs HCP, van Steenbergen JM and Kraayenhof R (1985) Studies on 9-amino-6-chloro-2-methoxy acridine fluorescence quenching and enhancement in relation to energy transduction in spheroplasts and intact cells of the cyanobacterium *Plectonema boryanum*. Photosynth Res 7: 59–67

Mohanty P, Srivastava M and Krishna KB (1997) The photosynthetic apparatus of *Spirulina*: electron transport and energy transfer. In: Vonshak A (ed) *Spirulina Platensis (Arthrospira)*, pp 17–42, Taylor & Francis, London

Papageorgiou GC (1996) The photosynthesis of cyanobacteria (blue bacteria) from the perspective of signal analysis of chlorophyll *a* fluorescence. J Sci Industr Res 55: 596–617

Peschek GA (1999) Photosynthesis and respiration of cyanobacteria: Bioenergetic significance and molecular interactions. In: Peschek GA, Löffelhardt W and Schmetterer G (eds) The Phototrophic Prokaryotes, pp 201–209. Kluwer Academic Publishers/Plenum Publishers, New York

Peschek GA, Nitschmann WH and Czerny T (1988) Respiratory proton extrusion and plasma membrane energization. Meth Enzymol 167: 361–379

Pils D and Schmetterer G (2001) Characterization of three bioenergetically active respiratory terminal oxidases in the cyanobacterium *Synechocystis* sp. strain PCC 6803. FEMS Microbiol Lett 203: 217–222

Pils D, Gregor W and Schmetterer G (1997) Evidence for *in vivo* activity of three distinct respiratory terminal oxidases in the cyanobacterium *Synechocystis* sp. strain PCC6803. FEMS Microbiol Lett 152: 83–88

Rakhimberdieva MG, Boichenko VA, Karapetyan NV and Stadnichuk IN (2001) Interaction of phycobilisomes with Photosystem II dimers and Photosystem I monomers and trimers in the cyanobacterium *Spirulina platensis*. Biochemistry 40: 15780–15788

Schlesinger P, Belkin S and Boussiba S (1996) Sodium deprivation under alkaline conditions causes rapid death of the filamentous cyanobacterium *Spirulina platensis*. J Phycol 32: 608–613

Schlösser UG (1994) SAG – Sammlung von Algenkulturen at the University of Göttingen. Catalogue of strains. Bot Acta 107: 113–186

Schmetterer G (1994) Cyanobacterial respiration. In: Bryant DG (ed) The Molecular Biology of Cyanobacteria, pp 409–435. Kluwer Academic Publishers, Dordrecht, The Netherlands

Shibata M, Katoh H, Sonoda M, Ohkawa H, Shimoyama M, Fukuzawa H, Kaplan A and Ogawa T (2002) Genes essential to sodium-dependent bicarbonate transport in cyanobacteria: Function and phylogenetic analysis. J Biol Chem 277: 18658–18664

Shubin VV, Tsuprun VL, Bezsmertnaya IN and Karapetyan NV (1993) Trimeric forms of the Photosystem I reaction center complex pre-exist in the membranes of the cyanobacterium *Spirulina platensis*. FEBS Lett 334: 79–82

Skulachev VP (1994) Chemiosmotic concept of the membrane bioenergetics: What is already clear and what is still waiting for elucidation? J Bioenerg Biomembr 26: 589–598

Teuber M, Rögner M and Berry S (2001) Fluorescent probes for non-invasive bioenergetic studies of whole cyanobacterial cells. Biochim Biophys Acta 1506: 31–46

Verma K and Mohanty P (2000) Changes of the photosynthetic apparatus in *Spirulina* cyanobacterium by sodium stress. Z Naturforsch [C] 55: 16–22

Vonshak A (1997) *Spirulina*: Growth, physiology and biochemistry. In: Vonshak A (ed) *Spirulina platensis (Arthrospira)*, pp 43–65. Taylor & Francis, London

Waditee R, Hibino T, Nakamura T, Incharoensakdi A and Takabe T (2002) Overexpression of a Na^+/H^+ antiporter confers salt tolerance on a freshwater cyanobacterium, making it capable of growth in sea water. Proc Natl Acad Sci USA 99: 4109–4114

Xu CH, Nejidat A, Belkin S and Boussiba S (1994) Isolation and characterization of the plasma membrane by two-phase partitioning from the alkalophilic cyanobacterium *Spirulina platensis*. Plant Cell Physiol 35: 737–741

Zeng MT and Vonshak A (1998) Adaptation of *Spirulina platensis* to salinity-stress. Comp Biochem Physiol A 120/121: 113–118